

文献

- 1) Yamakawa Y, Sata M, Suzuki H, et al. Higher elimination rate of hepatitis C virus among women. *J Viral Hepatitis* 3; 317-321, 1996.
- 2) Noguchi S, Sata M, Suzuki H, et al. Routes of transmission of hepatitis C virus in an endemic rural area of Japan. *Scand J Infect Dis* 29; 23-28, 1997.
- 3) Fukuizumi K, Sata M, Suzuki H, et al. Hepatitis C virus seroconversion rate in a hyperendemic area of HCV in Japan. a prospective study. *Scand J Infect Dis* 29; 345-347, 1997.
- 4) Fukuizumi K, Sata M, Suzuki H, et al. Natural disappearance of serum HCV RNA. prospective study in a hyperendemic area. *Hepatol Res* 9; 144-151, 1997.
- 5) Nagao Y, Sata M, Fukuizumi K, et al. High incidence of oral precancerous lesions in a hyperendemic area of hepatitis C virus infection. *Hepatol Res* 8; 173-177, 1997.
- 6) Sata M, Nakano H, Suzuki H, et al. Sero-epidemiologic study of hepatitis C virus infection in Fukuoka, Japan. *J Gastroenterol* 33; 218-222, 1998.
- 7) Sasaki K, Tajiri Y, Sata M, et al. *Helicobacter pylori* in the natural environment. *Scand J Infect Dis* 31; 275-279, 1999.
- 8) Toyonaga A, Okamatsu H, Sasaki K, et al. Epidemiological study on food intake and *Helicobacter pylori* infection. *Kurume Med J* 47; 25-30, 2000.
- 9) Nagao Y, Sata M, Fukuizumi K, et al. High incidence of oral lichen planus in HCV hyperendemic area. *Gastroenterology* 119; 882-883, 2000.
- 10) Nagao Y, Fukuizumi K, Tanaka K, et al. The prognosis for life in an HCV hyperendemic area. *Gastroenterology* 125; 628-629, 2003.
- 11) Nagao Y, Tanaka K, Kobayashi K, et al. A cohort study of chronic liver disease in an HCV hyperendemic area of Japan. a prospective analysis for 12 years. *Int J Mol Med* 13; 257-265, 2004.
- 12) Nagao Y, Tanaka K, Kobayashi K, et al. Analysis of approach to therapy for chronic liver disease in an HCV hyperendemic area of Japan. *Hepatol Res* 28; 30-35, 2004.
- 13) Kawaguchi T, Nagao Y, Tanaka K, et al. Causal relationship between hepatitis C virus core and the development of type 2 diabetes mellitus in a hepatitis C virus hyperendemic area. a pilot study. *Int J Mol Med* 16; 109-114, 2005.
- 14) Nagao Y, Kawaguchi T, Tanaka K, et al. Extrahepatic manifestations and insulin resistance in an HCV hyperendemic area. *Int J Mol Med* 16; 291-296, 2005.
- 15) Tanaka K, Nagao Y, Ide T, et al. Antibody to hepatitis B core antigen is associated with the development of hepatocellular carcinoma in hepatitis C virus-infected persons. a 12-year prospective study. *Int J Mol Med* 17; 827-832, 2006.
- 16) 長尾由実子、鈴木史雄、野林晴彦、他. 優れた薬物療法のさらなる普及をめざして－C型肝炎ウイルス感染者におけるインターフェロン療法の受療の現状と考察－. *リサーチペーパーシリーズ* 32; 1-181, 2006.
- 17) Nagao Y, Kawakami Y, Yoshiyama T, Sata M. Analysis of factors interfering with the acceptance of interferon therapy by HCV-infected patients. *Med Sci Monit* 14; 45-52, 2008.
- 18) Nagao Y, Tanaka J, Nakanishi T, et al. High incidence of extrahepatic manifestations in an HCV hyperendemic area. *Hepatol Res* 22; 27-36, 2002.
- 19) Nagao Y, Myoken Y, Katayama K, et al. Epidemiological survey of oral lichen planus

among HCV-infected inhabitants in a town in
Hiroshima Prefecture in Japan from 2000 to
2003. Oncol Rep 18; 1177- 1181, 2007.

著者連絡先：長尾 由実子
久留米大学医学部 消化器疾患情報講座
〒830-0011 久留米市旭町67

Received: 2009.12.21
Accepted: 2010.07.07
Published: 2011.02.01

Authors' Contribution:

- A** Study Design
- B** Data Collection
- C** Statistical Analysis
- D** Data Interpretation
- E** Manuscript Preparation
- F** Literature Search
- G** Funds Collection

The incidence of hepatocellular carcinoma associated with hepatitis C infection decreased in Kyushu area

Naota Taura^{1ABCDEF}, Nobuyoshi Fukushima^{2ABCDEF}, Hiroshi Yatsuhashi^{1ABCDEF}, Yuko Takami^{3ABCDEF}, Masataka Seike^{4ABCDEF}, Hiroshi Watanabe^{5ABCDEF}, Toshihiko Mizuta^{6ABCDEF}, Yutaka Sasaki^{7ABCDEF}, Kenji Nagata^{8ABCDEF}, Akinari Tabara^{9ABCDEF}, Yasuji Komorizono^{10ABCDEF}, Akinobu Taketomi^{11ABCDEF}, Shuichi Matsumoto^{12ABCDEF}, Tsutomu Tamai^{13ABCDEF}, Toyokichi Muro^{14ABCDEF}, Kazuhiko Nakao^{15ABCDEF}, Kunitaka Fukuizumi^{16ABCDEF}, Tatsuji Maeshiro^{17ABCDEF}, Osami Inoue^{18ABCDEF}, Michio Sata^{2ABCDEF}

- ¹ Clinical Research Center, National Nagasaki Medical Center, Omura City, Nagasaki, Japan
- ² Division of Gastroenterology, Department of Medicine, Kurume University School of Medicine, Kurume City, Fukuoka, Japan
- ³ Department of Surgery, National Hospital Organization Kyushu Medical Center, Chuo-ku, Fukuoka City, Fukuoka, Japan
- ⁴ 1st Department of Internal Medicine, Oita University Faculty of Medicine, Hasama-machi, Yufu City, Oita, Japan
- ⁵ Department of Hepatology, Fukuoka Red Cross Hospital, Minami-ku, Fukuoka City, Fukuoka, Japan
- ⁶ Department of Internal Medicine, Saga University Faculty of Medicine, Saga City, Saga, Japan
- ⁷ Department of Gastroenterology and Hepatology, Graduate School of Medical Sciences, Kumamoto University, Kumamoto City, Kumamoto, Japan
- ⁸ Department of Internal Medicine II, Miyazaki Medical College, Kiyotake-cho, Miyazaki-gun, Miyazaki, Japan
- ⁹ 3rd Department of Internal Medicine, University of Occupational and Environmental Health, Kitakyusyu City, Fukuoka, Japan
- ¹⁰ Department of Hepatology, Nanpuh Hospital, Kagoshima City, Kagoshima, Japan
- ¹¹ Department of Surgery and Science, Graduate school of medical sciences, Kyushu University, Fukuoka City, Fukuoka, Japan
- ¹² Department of Internal Medicine, Fukuoka Tokusyuikai Medical Center, Kasuga City, Fukuoka, Japan
- ¹³ Digestive Disease and Life-Style Related Disease, Health Research Human and Environmental Sciences, Kagoshima University, Kagoshima City, Kagoshima, Japan
- ¹⁴ Department of Gastroenterology, National Hospital Organization Oita Medical Center, Oita City, Oita, Japan
- ¹⁵ Department of Gastroenterology and Hepatology, Nagasaki University School of Medicine, Nagasaki City, Nagasaki, Japan
- ¹⁶ Department of Gastroenterology, National Hospital Organization, Kyushu Medical Center, Fukuoka City, Fukuoka, Japan
- ¹⁷ 1st Department of Internal Medicine, Faculty of Medicine, University of the Ryukyus, Nakagami-gun, Okinawa, Japan
- ¹⁸ Department of Gastroenterology, Nagasaki Rousai Hospital, Sasebo City, Nagasaki, Japan

Source of support: Departmental sources

Background:	Summary The incidence of hepatocellular carcinoma (HCC) in Japan has still been increasing. The aim of the present study was to analyze the epidemiological trend of HCC in the western area of Japan, Kyushu.
Material/Methods:	A total of 10,010 patients with HCC diagnosed between 1996 and 2008 in the Liver Cancer study group of Kyushu (LCSK), were recruited for this study. Cohorts of patients with HCC were categorized into five year intervals. The etiology of HCC was categorized to four groups as follows; B: HBsAg positive, HCV-RNA negative, C: HCV-RNA positive, HBsAg negative, B+C: both of HBsAg and HCV-RNA positive, non-BC: both of HBsAg and HCV-RNA negative.
Results:	B was 14.8% (1,485 of 10,010), whereas 68.1% (6,819 of 10,010) had C, and 1.4% (140 of 10,010) had HCC associated with both viruses. The remaining 1,566 patients (15.6%) did not associate with both viruses. Cohorts of patients with HCC were divided into six-year intervals (1996–2001 and 2002–2007). The ratio of C cases decreased from 73.1% in 1996–2001 to 64.9% in 2002–2007. On the other hand, B and nonBC cases increased significantly from 13.9% and 11.3% in 1996–2001 to 16.2% and 17.6% in 2002–2007, respectively.
Conclusions:	The incidence of hepatocellular carcinoma associated with hepatitis C infection decreased after 2001 in Kyushu area. This change was due to the increase in the number and proportion of the HCC not only nonBC patients but also B patients.
key words:	hepatitis virus • hepatocellular carcinoma • Japan
Full-text PDF:	http://www.medscimonit.com/fulltxt.php?ICID=881375
Word count:	1778
Tables:	3
Figures:	2
References:	32
Author's address:	Hiroshi Yatsuhashi, Clinical Research Center, National Nagasaki Medical Center, 2-1001-1 Kubara, Omura City, Nagasaki, Japan, e-mail: yatsuhashi@nmc.hosp.go.jp

PH

BACKGROUND

The three leading causes of death in Japan are malignancy neoplasms, cardiovascular diseases, and cerebrovascular diseases. Since 1981, malignant neoplasms have been the leading cause of death in Japan. For the last 30 years, liver cancer has been the third leading cause of death from malignant neoplasms in men. In women, liver cancer has ranked fifth during the past decade [1]. Hepatocellular carcinoma (HCC) accounts for 85% to 90% of primary liver cancers [2] and the age-adjusted HCC mortality rate has increased in recent decades in Japan [3]. Similarly, a trend of increasing rates of HCC has been reported from several developed countries in North America, Europe and Asia [4,5]. HCC often develops in patients with liver cirrhosis caused by hepatitis B virus (HBV), hepatitis C virus (HCV), excessive alcohol consumption, or nonalcoholic fatty liver disease. Of the hepatitis viruses which cause HCC, HCV is predominant in Japan [6–9].

Although the age-adjusted incidence of HCC has increased in Japan, sequential changes in etiology of HCC patients between 2001 and 2008 are not fully understood [10]. To clarify factors affecting epidemiological changes in Japanese HCC patients, especially the recent trend of HCC, we analyzed the epidemiological trend of HCC in the western area of Japan, Kyushu area.

MATERIAL AND METHODS

Patients

A total of 10,010 patients with HCC diagnosed between 1996 and 2008 in the Liver Cancer study group of Kyushu (LCSK), were recruited for this study. The diagnosis of HCC was based on AFP levels and imaging techniques including ultrasonography (USG), computerized tomography (CT), magnetic resonance imaging (MRI), hepatic angiography (HAG), and/or tumor biopsy. The diagnostic criteria for HCC were either a confirmative tumor biopsy or elevated AFP (>20 ng/mL) and neovascularization in HAG and/or CT.

Etiology of HCC

A diagnosis of chronic HCV infection was based on the presence of HCV-RNA detected by polymerase chain reaction (PCR), whereas diagnosis of chronic HBV infection was based on the presence of hepatitis B surface antigen (HBsAg). The etiology of HCC was categorized to four groups as follows; **B**: HBsAg positive, HCV-RNA negative, **C**: HCV-RNA positive, HBsAg negative, **B+C**: both of HBsAg and HCV-RNA positive, **nonBC**: both of HBsAg and HCV-RNA negative.

Statistical analysis

The data were analyzed by the Mann-Whitney test for the continuous ordinal data, the χ^2 test with Yates' correction and the Fisher exact test for the association between two qualitative variables. The standard deviation was calculated based on the binomial model for the response proportion. $P < 0.05$ was considered statistically significant.

RESULTS

Clinical features of the studied patients

A total of 10,010 patients with HCC were diagnosed at our study group from 1996 to 2008. Table 1 show that the proportion of patients diagnosed with **B** was 14.8% (1,485 of 10,010), whereas 68.1% (6,819 of 10,010) had **C**, and an additional 1.4% (140 of 10,010) had HCC associated with both viruses. The remaining 1,566 patients (15.6%) did not associate with both viruses. In analysis of patients in HCC by category, the median age of patients at diagnosis of **B** was 57 years old significant younger than other types HCC (**C**: 69, **nonBC**: 70, **B+C** 65 years old).

As shown in Figures 1 and 2, the number and ratio of **B** cases remained unchanged from 1996 to 2001 and thereafter increased and plateaued, whereas **C** rapidly increased from 1996 to 2000 and thereafter decreased and plateaued. In addition, the number and ratio of the **nonBC** cases has increased continued gradually and continued in this study period.

Change of etiology in patients with HCC during the period 1996–2007 with 6-years intervals

Cohorts of patients with HCC were divided into six-year intervals (1996–2001 and 2002–2007). Table 2 show that the incident rate of **C** decreased significantly from 73.1% in 1996–2001 to 64.9% in 2002–2007 (1996–2001 vs. 2002–2007, $p < 0.001$). On the other hand, the incident rate of **B** and **nonBC** increased significantly from 13.9% and 11.3% in 1996–2001 to 16.2% and 17.6% in 2002–2007, respectively. Not only the incident rate but also number of **B** and **nonBC** became larger in same 6 years periods.

Table 3 shows that male/female ratio of **C** and **nonBC** decreased significantly from 2.2 and 4.0 in 1996–2001 to 1.8 and 2.7 in 2002–2007, respectively ($p < 0.001$). The ratio became clearly smaller, indicates an increase in female patients with **C** and **nonBC**. On the other hand, the male/female ratio of **B** patients did not significantly change during the period. The median age at diagnosis of **B**, **C**, and **nonBC** in six-year intervals were significant increase from 56 to 58, from 67 to 71 and from 68 to 71 years of age during the period.

DISCUSSION

Our study was the twenty-three major liver center-based study designed to examine the sequential change in the background of HCC patients during the past 13 years, 1996–2008. More than 80% of our patients had chronic HBV or HCV infections. During this observation period, the number and proportion of HCC-C reached a peak in 2000 and thereafter decreased and became stabilized. Previous studies from Japan reported that the proportion of the HCC patients with HCV infection had been increased and reached a plateau in the period of 1981–2001 [1,3,10–12]. However, in our study, the number and proportion of the HCC patients with HCV infection cases decreased in 2001–2008. The reason may be explained as follows; interferon therapy for chronic hepatitis C may have been associated with a decreased incidence of HCC [13–17]. Oral supplementation with a oral branched-chain amino acids has been useful in the prevention HCC [18]. Finally, the chronically HCV-infected

Table 1. The characteristic of HCC patients during the period of 1996–2008.

Age (y.o.)	B		C		nonB		B+C		Total
	Male	Female	Male	Female	Male	Female	Male	Female	
0–	1	0	0	1	0	0	0	0	2
10–	4	1	0	0	0	2	0	0	7
20–	6	2	1	0	1	1	0	0	11
30–	31	5	4	0	11	3	2	0	56
40–	204	22	130	12	32	15	12	0	427
50–	507	66	728	145	167	32	31	6	1,682
60–	287	118	1836	741	411	102	35	13	3,543
70–	140	64	1775	947	483	133	22	14	3,578
80–	9	18	271	214	97	65	1	4	679
90–	0	0	9	5	9	2	0	0	58
Total	1,189	296	4,754	2,065	1,211	355	103	37	10,010
	1,485 (4.8%)		6,819 (68.1%)		1,566 (15.6%)		140 (1.4%)		
Median	57	63	67	70	68	70	61	68	67
	57		69		70		65		
Mean	56	64	68	71	69	71	62	68	67
	58		68		68		63		
Range	1–87	14–89	27–94	0–93	28–96	17–90	36–82	55–82	0–96
	1–89		0–94		17–96		36–82		

Age: B vs. C $p \leq 0.001$; B vs. B+C $p \leq 0.001$; B vs. nonBC $p \leq 0.001$; C vs. BC $p \leq 0.001$; C vs. nonBC $p = 0.043$; BC vs. nonB+C $p \leq 0.001$. IQR – interquartile range; SD – standard deviation.

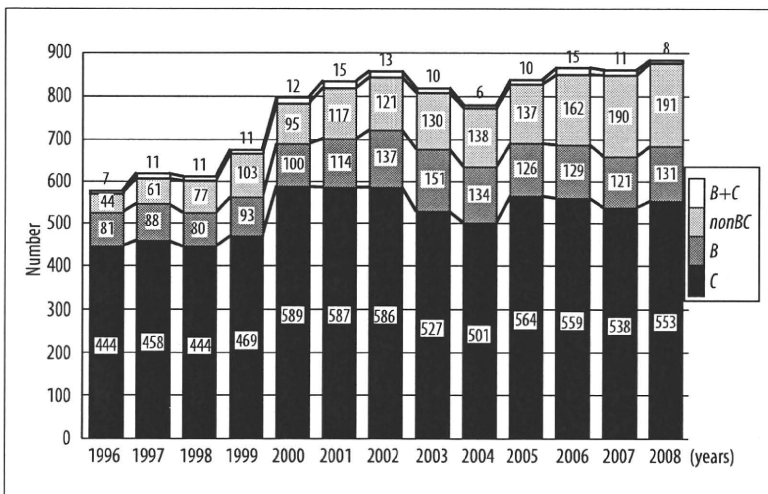


Figure 1. Sequential changes in the number of HCC patients categorized by etiology during the period 1996–2008.

population is aging in Japan. Yoshizawa et al. reported that age-specific prevalence for the presence of HCVAb among ~300,000 voluntary blood donors from Hiroshima in 1999 clearly increased with the age, reaching the highest proportion of 7% in individuals who were more than 70 years old [10,19]. In this study, the median age of the HCC patients with HCV infection steadily increased from 67 to 71 years of age during the studied period. In a word, HCV infected

people become older with years in Japan and they were regarded as a high risk for HCC.

The prevalence rate of HBV in Kyushu area has been reported to be higher than other area in Japan [1]. In Kyushu area, 95% of patients with chronic HBV infection had HBV genotype C except for Okinawa [20]. HBV genotype C is thought to be associated with higher incidence of HCC

PH

PERSONA ONLY

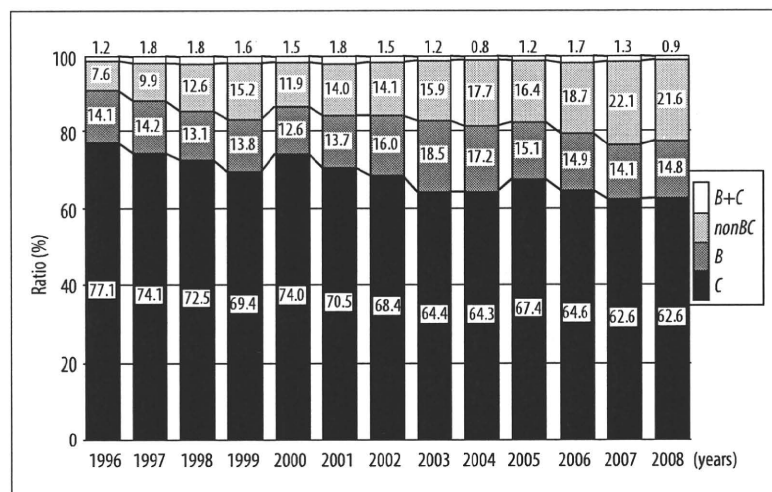


Figure 2. Sequential changes in the ratio of HCC patients categorized by etiology during the period 1996–2008.

Table 2. Change of etiology in patients with HCC during the period 1996–2007 with 6-years intervals.

Period	1996–2001	2002–2007	P value
Number	3,023	4,173	
Sex			
Male	2,162	2,849	
Female	861	1,324	
Ratio (male/female)	2.5	2.2	0.003
Age (y.o.) (IQR)	66 (14)	69 (12)	<0.001
Hepatitis virus (%)			
B	13.9	16.2	
C	73.1	64.9	
B+C	1.7	1.3	
nonBC	11.3	17.6	0.001

QR – interquartile range.

compared with other HBV genotypes [21]. In the present study, the incident rate of HCC patients with HBV infection became larger in this study period. To explain this change, we must consider from two viewpoints. The one is that the number of patients with HCC caused by HCV infection decreased, the other is that the proportion of chronic HBV infected patients who have reached the age of developing HCC is relatively high as described below.

Nationwide health survey for HBsAg in the over 40 years of age population had been done between 2002 and 2006 in Japan. This survey reports indicated that the average HBsAg prevalence was 1.2% in the total Japanese population patients with chronic HBV infection [10] and the age-specific prevalence of HBsAg was higher in the group aged between 50 (1.4%) and 55 years (1.5%). In the HCC patients with HBV genotype C, the mean age was 55 years in Japan [20]. This overlap between age-specific prevalence and hepatocellular carcinogenic age would be associated with the increase of HCC patients with HBV infection. Nucleoside analogue reverse transcriptase inhibitor (NARTI) therapy effectively reduces the incidence of HCC in chronic hepatitis B patients [22,23]. However, Interferon therapy for

Table 3. The median age and male/female ratio of HCC patients during the period of 1996–2007.

Period	1996–2001	2002–2007	P value
B			
Age (y.o.) (IQR)	56 (14)	58 (15)	0.001
Sex			
Male	331	519	
Female	88	157	
Ratio (male/female)	3.8	3.3	0.391
C			
Age (y.o.) (IQR)	67 (9)	71 (11)	<0.001
Sex			
Male	1,524	1,753	
Female	687	955	
Ratio (male/female)	2.2	1.8	0.002
nonBC			
Age (y.o.) (IQR)	68 (12)	71 (13)	<0.001
Sex			
Male	273	534	
Female	69	201	
Ratio (male/female)	4.0	2.7	0.012

QR – interquartile range.

chronic hepatitis C started from 1992, whereas NARTI therapy for HBV started from 2000 in Japan [24,25]. Hence, HBV associated HCC will probably decrease in Japan during the next 10 to 20 years.

The survey of HCC patients associated with nonBC infection in Japan was conducted by Inuyama Hepatitis Research Group from 1995 to 2003. The ratio of HCC patients with nonBC accounted 9.3% [1]. In the present study, the ratio of HCC patients with nonBC was 14.1%. Furthermore, the number and the proportion of HCC patients with nonBC have been gradually increasing in the periods. The current two studies account for the increase in number and proportion of HCC patients with nonBC. First, Lai et al. reported

that type 2 diabetes increases the risk of developing HCC in those who are HCV negative or have a high level of total cholesterol [26]. Second, Nakano et al. reported that epidemiological studies on diabetes mellitus revealed that the number of patients with diabetes mellitus is gradually increasing in Japan along with development of car society and westernization of food intake. Since prevalence of diabetes mellitus increases with aging, proportion of individuals with diabetes mellitus aged over 60 has exceeded two-third of estimated total number of patients (7.40 million in 2002) in Japan where aging of society is rapidly progressing [27]. In a word, the number of type 2 diabetes people is increasing in Japan and they were regarded as a high risk for HCC. Then, the number and the proportion of HCC patients with nonBC have been increased recent twelve years in Japan.

It is known that 2 to 4 decades of chronic HCV infection are required to develop cirrhosis and subsequent HCC [28–31]. The number of HCC cases has increased in Japan, because individuals infected with HCV during the past have grown old and have reached the cancer-bearing age. The prevalence of HCV infection in young Japanese individuals is low and the incidence of HCVAb is very low because of preventative actions against HCV infection such as the screening of blood products for HCV and the use of sterile medical equipment [32]. Additionally, we showed that the number and proportion of patients with HCC-C cases decreased, whereas the number and ratio of HCC-nonBC steadily increased during the studied period. These findings may be expected that the incidence of HCC patients with nonBC in Japan may continue to increase even after the consequence of the HCV epidemic level off, a country that is far advanced with regard to HCC patients with HCV infection, in the near future.

CONCLUSIONS

In summary, HCC patients had increased from 1996 to 2000 and this increase was originated from HCC patients with HCV infection. The number and proportion of HCC patients with HCV infection reached a peak in 2000 and thereafter decreased and became stabilized. The incidence of hepatocellular carcinoma associated with hepatitis C infection decreased after 2001 in Kyushu area. This change was due to the increase in the number and proportion of the HCC not only nonBC patients but also B patients.

REFERENCES:

- Umamura T, Kiyosawa K: Epidemiology of hepatocellular carcinoma in Japan. *Hepatol Res*, 2007; 37(Suppl.2): S95–100
- El-Serag HB, Rudolph KL: Hepatocellular carcinoma: epidemiology and molecular carcinogenesis. *Gastroenterology*, 2007; 132: 2557–76
- Kiyosawa K, Tanaka E: Characteristics of hepatocellular carcinoma in Japan. *Oncology*, 2002; 62: 5–7
- McGlynn KA, Tsao L, Hsing AW et al: International trends and patterns of primary liver cancer. *Int J Cancer*, 2001; 94: 290–96
- Bosch FX, Ribes J, Diaz M, Cleries R: Primary liver cancer: worldwide incidence and trends. *Gastroenterology*, 2004; 127: S5–16
- Hamasaki K, Nakata K, Tsutsumi T et al: Changes in the prevalence of hepatitis B and C infection in patients with hepatocellular carcinoma in the Nagasaki Prefecture, Japan. *J Med Virol*, 1993; 40: 146–49
- Kato Y, Nakata K, Omagari K et al: Risk of hepatocellular carcinoma in patients with cirrhosis in Japan. Analysis of infectious hepatitis viruses. *Cancer*, 1994; 74: 2234–38
- Shiratori Y, Shiina S, Imamura M et al: Characteristic difference of hepatocellular carcinoma between hepatitis B- and C- viral infection in Japan. *Hepatology*, 1995; 22: 1027–33
- Shiratori Y, Shiina S, Zhang PY et al: Does dual infection by hepatitis B and C viruses play an important role in the pathogenesis of hepatocellular carcinoma in Japan? *Cancer*, 1997; 80: 2060–67
- Kiyosawa K, Umamura T, Ichijo T et al: Hepatocellular carcinoma: recent trends in Japan. *Gastroenterology*, 2004; 127: S17–26
- Taura N, Yatsuhashi H, Hamasaki K et al: Increasing hepatitis C virus-associated hepatocellular carcinoma mortality and aging: Long term trends in Japan. *Hepatol Res*, 2006; 34: 130–34
- Taura N, Hamasaki K, Nakao K et al: Aging of patients with hepatitis C virus-associated hepatocellular carcinoma: long-term trends in Japan. *Oncol Rep*, 2006; 16: 837–43
- Nishiguchi S, Kuroki T, Nakatani S et al: Randomised trial of effects of interferon-alpha on incidence of hepatocellular carcinoma in chronic active hepatitis C with cirrhosis. *Lancet*, 1995; 346: 1051–55
- Nishiguchi S, Shiomi S, Nakatani S et al: Prevention of hepatocellular carcinoma in patients with chronic active hepatitis C and cirrhosis. *Lancet*, 2001; 357: 196–97
- Kasahara A, Hayashi N, Mochizuki K et al: Risk factors for hepatocellular carcinoma and its incidence after interferon treatment in patients with chronic hepatitis C. Osaka Liver Disease Study Group. *Hepatology*, 1998; 27: 1394–402
- Ikeda K, Saitoh S, Arase Y et al: Effect of interferon therapy on hepatocellular carcinogenesis in patients with chronic hepatitis type C: A long-term observation study of 1,643 patients using statistical bias correction with proportional hazard analysis. *Hepatology*, 1999; 29: 1124–30
- Makiyama A, Itoh Y, Kasahara A et al: Characteristics of patients with chronic hepatitis C who develop hepatocellular carcinoma after a sustained response to interferon therapy. *Cancer*, 2004; 101: 1616–22
- Muto Y, Sato S, Watanabe A et al: Effects of oral branched-chain amino acid granules on event-free survival in patients with liver cirrhosis. *Clin Gastroenterol Hepatol*, 2005; 3: 705–13
- Yoshizawa H: Hepatocellular carcinoma associated with hepatitis C virus infection in Japan: projection to other countries in the foreseeable future. *Oncology*, 2002; 62: 8–17
- Orito E, Mizokami M: Hepatitis B virus genotypes and hepatocellular carcinoma in Japan. *Intervirology*, 2003; 46: 408–12
- Orito E, Mizokami M: Differences of HBV genotypes and hepatocellular carcinoma in Asian countries. *Hepatol Res*, 2007; 37: S33–35
- Matsumoto A, Tanaka E, Rokuhara A et al: Efficacy of lamivudine for preventing hepatocellular carcinoma in chronic. *Hepatol Res*, 2005; 32(3): 173–84
- Xu J, Shi J, Wang YP et al: Milder liver cirrhosis and loss of serum HBeAg do not imply lower risk for. *Med Sci Monit*, 2009; 15(6): CR274–79
- Hayashi N, Takehara T: Antiviral therapy for chronic hepatitis C: past, present, and future. *J Gastroenterol*, 2006; 41(1): 17–27
- Kumashiro R, Kuwahara R, Ide T et al: Subclones of drug-resistant hepatitis B virus mutants and the outcome of breakthrough hepatitis in patients treated with lamivudine. *Intervirology*, 2003; 46(6): 350–54
- Lai MS, Hsieh MS, Chiu YH, Chen TH: Type 2 diabetes and hepatocellular carcinoma: A cohort study in high prevalence area of hepatitis virus infection. *Hepatology*, 2006; 43: 1295–302
- Nakano T, Ito H: Epidemiology of diabetes mellitus in old age in Japan. *Diabetes Res Clin Pract*, 2007; 77(Suppl.1): S76–81
- Deuffic S, Poynard T, Valleron AJ: Correlation between hepatitis C virus prevalence and hepatocellular carcinoma mortality in Europe. *J Viral Hepat*, 1999; 6: 411–13
- El-Serag HB, Mason AC: Rising incidence of hepatocellular carcinoma in the United States. *N Engl J Med*, 1999; 340: 745–50
- Planas R, Balleste B, Antonio Alvarez M et al: Natural history of decompensated hepatitis C virus-related cirrhosis. A study of 200 patients. *J Hepatol*, 2004; 40: 823–30
- Davila JA, Morgan RO, Shaib Y et al: Hepatitis C infection and the increasing incidence of hepatocellular carcinoma: a population-based study. *Gastroenterology*, 2004; 127: 1372–80
- Sasaki F, Tanaka J, Moriya T et al: Very low incidence rates of community-acquired hepatitis C virus infection in company employees, long-term inpatients, and blood donors in Japan. *J Epidemiol*, 1996; 6: 198–203

PH

Contrast-Enhanced Ultrasound With Perflubutane Microbubble Agent: Evaluation of Differentiation of Hepatocellular Carcinoma

Masanori Takahashi¹
Hitoshi Maruyama
Hiroyuki Ishibashi
Masaharu Yoshikawa
Osamu Yokosuka

OBJECTIVE. The aim of this study was to evaluate the effectiveness of contrast-enhanced ultrasound with a perflubutane microbubble agent in the assessment of cellular differentiation of hepatocellular carcinoma (HCC).

SUBJECTS AND METHODS. Continuous harmonic imaging with a low mechanical index (0.21–0.30) was performed 1, 5, and 10 minutes after IV contrast injection (0.0075 mL/kg). Tumor enhancement was evaluated by both subjective reading and objective intensity analysis based on the signal distribution in the nontumor parenchyma. Tumor vascularity was assessed with CT during hepatic arteriography.

RESULTS. Sixty-four patients with 77 histologically proved HCCs (mean greatest dimension, 19.1 ± 5.3 mm)—six poorly differentiated HCCs, 45 moderately differentiated HCCs, and 26 well-differentiated HCCs—were enrolled in this prospective study. Among 64 hyperenhancing lesions on peak enhancement sonograms, four poorly differentiated HCCs and eight moderately differentiated HCCs exhibited washout within 1 minute. In addition to these 12 lesions, 36 lesions exhibited washout 5 minutes after injection, resulting in a total of 48 washout lesions. Fifty-four lesions exhibited washout 10 minutes after contrast injection (six poorly differentiated, 38 moderately differentiated, and 10 well-differentiated HCCs). Washout was more frequent in poorly than in moderately differentiated HCC ($p = 0.0117$) and well-differentiated HCC ($p = 0.0003$) in the 1-minute phase and was more frequent in moderately differentiated than in well-differentiated HCC in the 5-minute ($p = 0.0026$) and 10-minute ($p = 0.0117$) phases. Thirteen lesions were isoenhancing or hypoenhancing on peak enhancement sonograms (three moderately differentiated and 10 well-differentiated HCCs). Contrast-enhanced ultrasound and CT during hepatic arteriography did not differ significantly with respect to rate of detection of hyperenhancing lesions.

CONCLUSION. The findings at contrast-enhanced ultrasound with the perflubutane microbubble agent may be predictive of cellular differentiation of HCC without needle biopsy.

Keywords: cellular differentiation, contrast agent, hepatocellular carcinoma, liver, ultrasound

DOI:10.2214/AJR.10.4242

Received January 5, 2010; accepted after revision July 12, 2010.

¹All authors: Department of Medicine and Clinical Oncology, Chiba University Graduate School of Medicine, 1-8-1, Inohana, Chuo-ku, Chiba 260-8670, Japan. Address correspondence to H. Maruyama (maru-cib@umin.ac.jp).

WEB

This is a Web exclusive article.

AJR 2011; 196:W123–W131

0361–803X/11/1962–W123

© American Roentgen Ray Society

Hepatocellular carcinoma (HCC) is one of the most common forms of cancer worldwide, especially in the eastern part of Asia [1]. Although the results of therapy for HCC have improved remarkably, the prognosis among patients with cirrhosis continues to depend on the rates of occurrence and progression of this tumor [2]. Hypervascularity is a known characteristic imaging finding of HCC [3–6] and an important marker in differential diagnosis. Hypervascularity, however, is a result of dedifferentiation, and some early-stage HCCs appear as isovascular or hypovascular lesions [7–10]. Contrast imaging techniques have become extensively used to assess the vascularization and cellular differentiation of HCC.

With ultrasound, real-time and repeated observation can be performed, and ultrasound is more convenient than CT and MRI. With the development of microbubble contrast agents, the diagnostic utility of ultrasound has increased substantially [11–15]. The perflubutane microbubble ultrasound contrast agent (Sonazoid, GE Healthcare) accumulates in the reticuloendothelial system, such as in the Kupffer cells [16, 17]. As cellular differentiation in HCC progresses from a nontumor tissue-like appearance to well-differentiated cancerous tissue [18–20], the difference in contrast enhancement between the HCC lesion and adjacent liver parenchyma at perflubutane microbubble-enhanced ultrasound may indicate the grade of cellular differentiation of HCC. The results of one study

[21] showed the usefulness of ultrasound enhanced with perflubutane microbubbles in comparison with superparamagnetic iron oxide-enhanced MRI in estimation of the histologic grade of HCC. The results of that study were based on imaging findings represented by accumulation of the microbubbles of the perflubutane agent. However, contrast enhancement may be closely related to the dynamic behavior of the microbubbles while the agent circulates. For this reason, we designed a study to objectively examine phase-related changes in contrast enhancement in signal intensity analysis. The aim of this study was to clarify the clinical efficacy of ultrasound enhanced with perflubutane microbubble contrast material in the noninvasive assessment of cellular differentiation of HCC.

Subjects and Methods

Patients

From February 2007 through September 2009, this prospective study was conducted with the following inclusion criteria: patient has cirrhosis and one or more hepatic lesions smaller than 30 mm in maximum diameter found with unenhanced gray-scale ultrasound, contrast-enhanced ultrasound of the hepatic lesion is scheduled, CT during hepatic arteriography (CTHA) to assess the vascularity of the hepatic lesion is scheduled for less than 2 weeks after the contrast-enhanced ultrasound examination, percutaneous liver biopsy or open resection of the hepatic lesion is scheduled, and the patient has no contraindications to administration of perflubutane microbubble contrast agent, that is, egg allergy and severe pulmonary or cardiac disease. The histologic diagnosis of HCC lesions was made by analysis of the specimen obtained at surgery or ultrasound-guided needle biopsy with a 21-gauge needle (Sonopsy-C1, Hakko) after the contrast-enhanced ultrasound examination. This study was approved by the ethics committee of our institute, and informed written consent was obtained from all patients.

Ultrasound Examination

Ultrasound examinations (SSA-770A or 790A Aplio system, Toshiba) were performed with a 3.75-MHz convex probe. First, unenhanced gray-scale ultrasound imaging (tissue harmonic imaging, 2.5/5.0 Hz) was performed to observe the tumor appearance and to measure the maximum diameter of the nodule. The scan plane that allowed the most suitable depiction of the HCC lesion was carefully selected. Second, color Doppler ultrasound was used to evaluate the vascular abnormality within and around the tumor area. Third, contrast-enhanced ultrasound examina-

tions were performed in harmonic imaging mode with a low mechanical index (0.21–0.30) chosen on the basis of a previous report [13]. The focal point was set at the deepest level of the HCC lesion. Gain was adjusted at an optimal level, and the dynamic range was set at 60–65 dB for unenhanced gray-scale ultrasound and 40–50 dB for contrast-enhanced ultrasound. These settings were used in all ultrasound examinations.

The perflubutane microbubble contrast agent (median bubble diameter, 2–3 μm) was administered to all patients at a dose of 0.0075 mL/kg by manual bolus injection followed by a flush of 5.0 mL normal saline solution through an antecubital or cubital vein. In cases of multiple hepatic lesions, the contrast agent was injected for observation of each lesion, and the additional injection was performed after the previous enhancement disappeared. After injection of the contrast agent, ultrasound images of the HCC lesion were obtained in the first minute by continuous scanning (15 Hz). Next, 5- and 10-minute phase images were obtained for a few seconds in each phase. Ultrasound examinations were conducted by three experts in hepatology and radiology (8, 8, and 20 years of experience in ultrasound examination). All images acquired were recorded digitally and reviewed at a later date by the observer with 20 years of experience, who was blinded to the clinical background of the patients. Contrast enhancement of HCC lesions was qualitatively assessed in each phase by comparison with enhancement of the adjacent liver parenchyma and classified as hyperenhancement, iso-enhancement, or hypo-enhancement.

Quantitative Assessment of Contrast-Enhanced Ultrasound Findings

Specialized software for intensity analysis (ImageLab, Toshiba) was used in this study (Fig. 1). First, a region of interest (ROI) was set manually on the whole HCC lesion on contrast-enhanced sonograms obtained during the first minute after contrast injection, and the time to reach the peak enhancement of the HCC lesion was measured on the time-intensity curve. Second, two ROIs the same size of the HCC lesion were set on the HCC lesion and adjacent liver parenchyma for calculation of the differences in intensity in the four phases: peak enhancement and 1, 5, and 10 minute after injection. Next, with an ROI the same size as the average diameter of the HCC lesion, the variability of contrast enhancement over the nontumor liver parenchyma was examined to obtain the reference value for assessment of contrast enhancement of the HCC lesion.

Three ROIs were set side by side on nontumor liver parenchyma at the same depth from the skin surface on the contrast-enhanced sonograms,

and maximum differences in intensity among the three ROIs were calculated in the four phases. The average value of maximum intensity difference of nontumor liver parenchyma was calculated in each phase and defined as the intensity distribution in nontumor liver parenchyma. If the intensity difference between the HCC lesion and adjacent liver parenchyma was greater than the range of intensity distribution in nontumor liver parenchyma, the tumor finding was defined as hyperenhancement or hypo-enhancement. If the intensity difference between the HCC lesion and adjacent liver parenchyma was within the range of the intensity distribution in nontumor liver parenchyma, the tumor finding was defined as iso-enhancement. Washout in the HCC lesion was considered present when hyperenhancement or iso-enhancement at peak enhancement shifted to hypo-enhancement, and the presence or absence of washout was assessed in each phase.

One of the observers with 8 years of experience performed ROI positioning for the data used for the results. In addition, interobserver and intraobserver variability of intensity results for ROI positioning was examined with the ROI positioned by the other observer with 8 years of experience. Although we compared intensity-based and reading-based results, contrast enhancement of the tumor in this study was defined by the results of the intensity-based assessment.

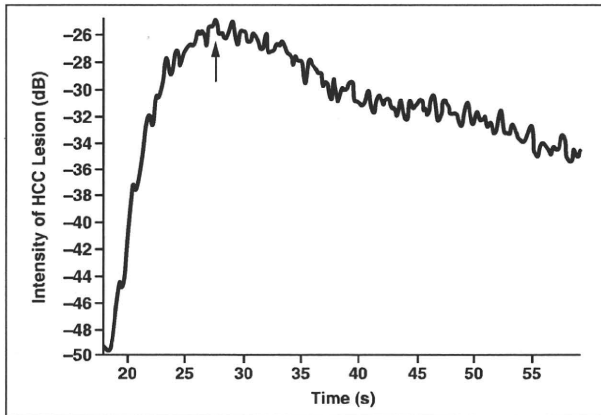
CT During Hepatic Arteriography

CTHA was performed with an interventional radiology-CT system (Infinix Activ, Toshiba) after injection of 15 mL of iodinated contrast medium (iopamidol, Iopamiron 300, Bayer Schering Pharma) by mechanical power injector at a rate of 3 mL/s through a catheter placed in the common hepatic artery. For the arterial phase, images were obtained at 3 and 15 seconds after contrast administration. An expert in hepatology and radiology with 30 years of experience, who was blinded, evaluated the CTHA findings on the HCC lesions by comparing them with adjacent liver parenchyma and describing the appearance as hyperenhancement, iso-enhancement, or hypo-enhancement.

Statistical Analysis

All data are expressed as the mean \pm SD or percentage. Statistically significant differences between contrast-enhanced ultrasound and CTHA with respect to detectability of tumor vascularity were examined by chi-square test. Agreement of contrast-enhanced ultrasound findings between intensity-based and reading-based assessment was examined with kappa statistics. A kappa value up to 0.2 indicated poor agreement; 0.2–0.4, slight agreement; 0.4 to 0.6, moderate agreement; 0.6

Ultrasound of Hepatocellular Carcinoma



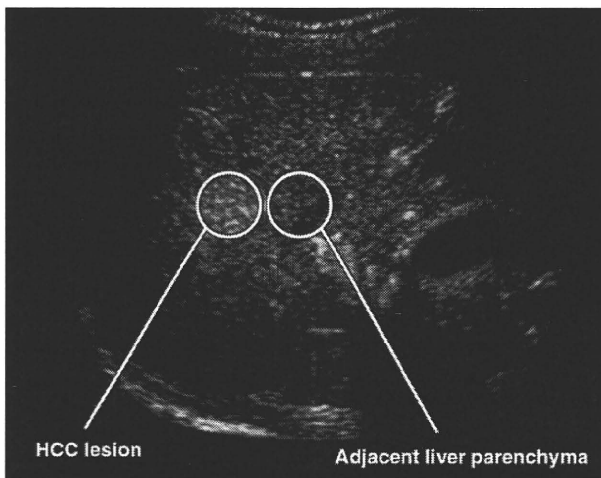
A

Fig. 1—Quantitative assessment of contrast-enhanced ultrasound findings of hepatocellular carcinoma (HCC).

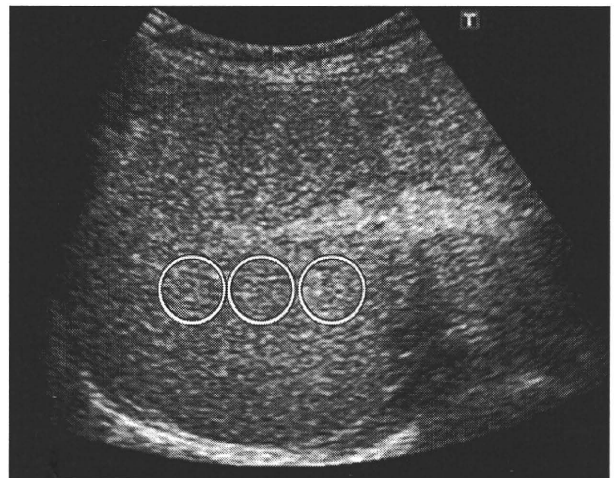
A. Time-intensity curve for HCC lesion shows peak enhancement of nodule occurred 28 seconds (arrow) after contrast injection.

B. 64-year-old man with hepatitis C-related cirrhosis. Contrast-enhanced ultrasound image shows intensity-based quantitative assessment of contrast enhancement in HCC lesion. Two regions of interest (circles) were set at HCC lesion and adjacent liver parenchyma for calculation of difference in intensity between them.

C. Contrast-enhanced ultrasound image in same patient shows analysis of intensity distribution in nontumor liver parenchyma. Three regions of interest (circles) were set side by side in nontumor liver parenchyma at same depth from skin surface, and maximum difference in intensity among three regions of interest was calculated. In this way, average of maximum differences was calculated at peak enhancement and in 1-, 5-, and 10-minute phases as intensity distribution of nontumor liver parenchyma. If intensity difference between HCC lesion and adjacent liver parenchyma was greater than range of intensity distribution in nontumor liver parenchyma, tumor finding was defined as hyperenhancing or hypoenhancing. If intensity difference between HCC lesion and adjacent liver parenchyma was within range of intensity distribution in nontumor liver parenchyma, tumor finding was defined as isoenhancing.



B



C

to 0.8, good agreement; and greater than 0.8, excellent agreement. The relation between the frequency of washout after peak enhancement and cellular differentiation of HCC was examined by chi-square test followed by multiple comparison performed with the Ryan procedure. Interobserver and intraobserver variability of intensity results for positioning ROIs was examined with coefficient of variation ($SD/mean \times 100$). The level of statistical significance was set at $p < 0.05$. Statistical analysis was performed with an SPSS software package (version 13.0 J, SPSS).

Results

Clinical Background

The 99 patients who met the inclusion criteria had 113 lesions; however, 27 lesions in 26 patients were excluded because the histologic diagnosis of 16 lesions was other than HCC (seven adenocarcinomas, nine benign nodules) and an insufficient amount of tissue was obtained from the other 11 lesions. In ad-

dition, nine lesions in nine patients that had a nodule-in-nodule CTHA appearance were excluded because two different pathologic components might have been present in the nodules. Therefore, we evaluated 77 HCC lesions (diameter, 19.1 ± 5.3 mm; range, 9.2–29.5 mm) in 64 patients (50 men, 14 women; mean age, 66.5 ± 9.6 years; range, 41–86 years). All 64 patients had cirrhosis. Four diagnoses of cirrhosis were based on the results of pathologic examination, and 60 were based on imaging findings, biochemical findings, and clinical symptoms. The cause of cirrhosis was hepatitis B virus infection in 13 patients, hepatitis C virus infection in 42 patients, alcohol abuse in five patients, autoimmune hepatitis in one patient, primary biliary cirrhosis in one patient, and cryptogenic processes in two patients.

The total number of HCC lesions was one in 52 patients, two in 11 patients, and three in one patient. The unenhanced gray-scale ul-

trasound pattern of 24 HCC lesions was hyperechoic, 10 lesions was isoechoic, 37 lesions was hypoechoic, and six lesions was heterogeneous. The histologic diagnosis of three HCC lesions was made with a surgical specimen and of 74 lesions was made after ultrasound-guided needle biopsy. Six HCC lesions were poorly differentiated; 45 lesions, moderately differentiated; and 26 lesions, well-differentiated. All the patients underwent surgery or biopsy within 2 weeks after contrast-enhanced ultrasound examination. The serum α -fetoprotein levels ranged from 1.8 to 1,266.1 ng/mL. The level was normal in 21 patients and abnormal in 43 patients (111.9 ± 240.0 ng/mL).

Contrast-Enhanced Ultrasound Findings at Peak Enhancement

The time-intensity analysis revealed that all HCC lesions exhibited peak enhancement within 1 minute after contrast injection. The

variability of contrast enhancement over the nontumor liver parenchyma in this phase was examined in 16 patients in whom three ROIs could be set side by side on nontumor liver parenchyma. The ultrasound plane of the liver in the other 48 patients did not have enough area for the three ROIs owing to the presence of relatively large intrahepatic vessels. Because the intensity distribution in nontumor liver parenchyma was 2.2 ± 0.6 dB, 64 lesions (83.1%) with an intensity difference of 10.0 ± 5.3 dB (range, 2.3–22.6 dB) between the lesions and adjacent liver parenchyma were classified as hyperenhancing. Similarly, 11 lesions (14.3%) with an intensity difference of 0.3 ± 1.2 dB (range, -2.0 to 1.9 dB) were classified as iso-enhancing, and two lesions (2.6%) with an intensity difference of -5.9 ± 0.9 dB (range, -6.5 to -5.2 dB) were classified as hypo-enhancing.

The interobserver and intraobserver variability of intensity results for ROI positioning was 4.7% and 3.1% for HCC lesions and 5.6% and 2.8% for nontumor hepatic parenchyma. Excellent agreement was found between in-

TABLE 1: Concordance Between Contrast-Enhanced Ultrasound and CT During Hepatic Arteriography With Respect to Enhancement of Hepatocellular Carcinoma (n = 77)

CT During Hepatic Arteriography	Contrast-Enhanced Ultrasound	
	Hyperenhancement	Isoenhancement or Hypoenhancement
Hyperenhancement	63	0
Isoenhancement or hypoenhancement	1	13

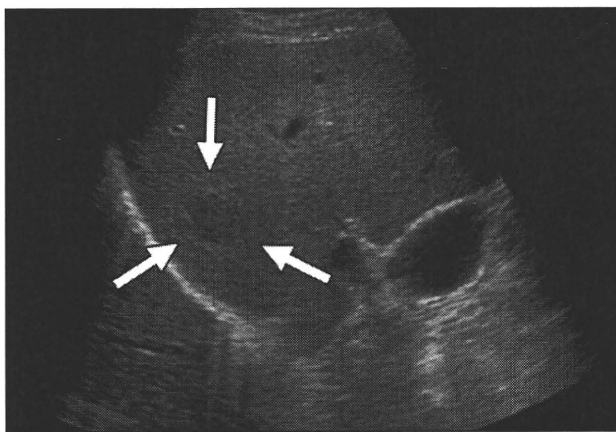
Note— $p = 0.8553$.

tensity-based and reading-based assessment ($\kappa = 0.912$), although there were two cases of disagreement. One lesion was found to be iso-enhancing according to reading-based assessment and hyperenhancing by intensity-based assessment. The other lesion was found iso-enhancing by reading-based assessment and hypo-enhancing by intensity-based assessment. Because CTHA showed hypervascularity in 63 of 77 lesions (81.8%), the concordance rate between contrast-enhanced ultrasound and CTHA with respect to hyperenhancement was 98.4% (63/64; Table 1 and Fig. 2). The detectability of tumor vascularity

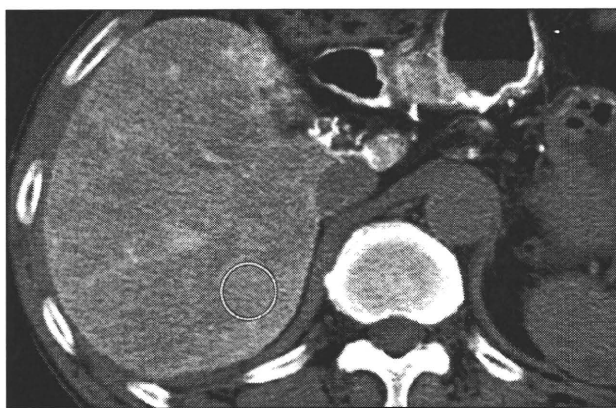
was not significantly different between these two modalities ($p = 0.8553$).

Washout Time After Peak Enhancement

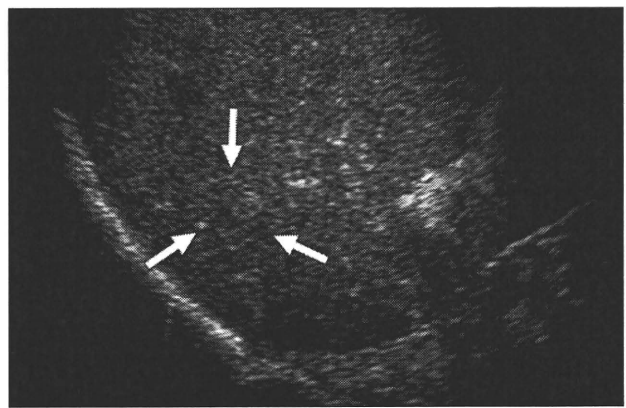
In a procedure similar to that for the peak enhancement phase, the variability of contrast enhancement over the nontumor liver parenchyma 1, 5, and 10 minutes after contrast injection was examined in 16 patients. The findings were 1.6 ± 0.6 dB (range, 0.4–3.0 dB) in the 1-minute phase, 1.5 ± 0.4 dB (range, 0.8–2.2 dB) in the 5-minute phase, and 1.3 ± 0.5 dB (range, 0.3–2.0 dB) in the 10-minute phase. In total, 54 of the 64 lesions with hyperenhancement in the peak enhancement phase exhibited washout. In the 1-minute phase, 12 lesions exhibited an intensity difference of -5.9 ± 0.9 dB (range, -6.5 to -5.2 dB) between HCC lesions and adjacent liver parenchyma. In the 5-minute



A



B



C

Fig. 2—72-year-old man with hepatitis C-related cirrhosis. **A**, Unenhanced sonogram shows 17.0-mm-diameter hypoechoic lesion (arrows) in liver. **B**, CT scan during hepatic arteriography obtained 15 seconds after contrast administration shows iso-enhancing lesion (circle). **C**, Contrast-enhanced sonogram at peak enhancement (35 seconds after agent injection) shows hyperenhancement (arrows) in lesion, which was diagnosed as moderately differentiated hepatocellular carcinoma after ultrasound-guided needle biopsy.

TABLE 2: Relation Between Cellular Differentiation of Hyperenhancing Hepatocellular Carcinoma at Peak Enhancement (n = 64) and Phase at Which Washout Occurred

Differentiation	1-Minute Phase	5-Minute Phase	10-Minute Phase
Poor (n = 6)	4 (66.7) ^{a,b}	6 (100)	6 (100)
Moderate (n = 42)	8 (19.0) ^a	35 (83.3) ^c	38 (90.5) ^d
Well (n = 16)	0 (0) ^b	7 (43.8) ^c	10 (62.5) ^d

Note—Values are number of hepatocellular carcinoma lesions with percentages in parentheses.

^ap = 0.0117.

^bp = 0.0003.

^cp = 0.0026.

^dp = 0.0117.

phase, 48 lesions exhibited an intensity difference of -4.4 ± 1.7 dB (range, -7.3 to -1.9 dB). In the 10-minute phase, 54 lesions exhibited an intensity difference of -5.3 ± 2.4 dB (range, -16.2 to -1.9 dB). The other 10 lesions, which had an intensity difference of -0.6 ± 0.6 dB (range, -1.0 to 0.5 dB), were classified as iso-enhancing in the 10-minute phase. The 13 lesions that were iso-enhancing or hypo-enhancing at peak enhancement had an intensity difference of -0.3 ± 0.7

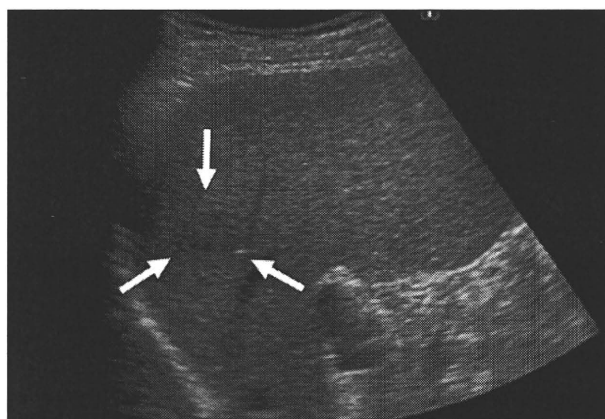
dB (range, -1.2 to 0.8 dB) in the 10-minute phase. Therefore, these 23 lesions did not exhibit washout during enhancement.

The contrast-enhanced ultrasound findings obtained at intensity-based and reading-based assessment exhibited excellent agreement in all three phases after peak enhancement: kappa values of 0.847 for the 1-minute phase, 0.915 for the 5-minute phase, and 0.970 for the 10-minute phase. All seven cases of disagreement about the 1-, 5-, and

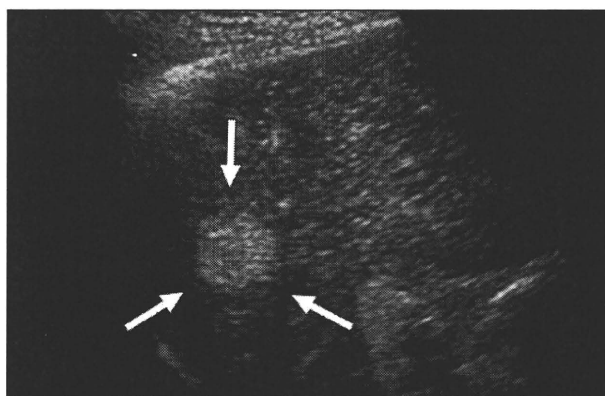
10-minute phase images were lesions that were iso-enhancing by reading-based assessment and hypo-enhancing by intensity-based assessment. The interobserver and intraobserver variability of intensity results for positioning ROIs was calculated in each phase. The results were 6.2% and 4.0% for HCC lesions and 5.6% and 4.7% for nontumor liver parenchyma in the 1-minute phase, 8.0% and 5.8% for HCC lesions and 7.4% and 3.4% for nontumor liver parenchyma in the 5-minute phase, and 7.4% and 5.7% for HCC lesions and 7.9% and 5.6% for nontumor liver parenchyma in the 10-minute phase.

Relation Between Contrast-Enhanced Ultrasound Findings on HCC Lesions and Cellular Differentiation

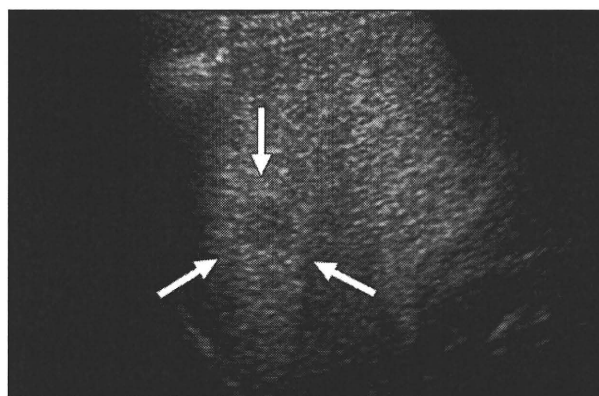
Among 64 lesions hyperenhancing at peak enhancement, four poorly differentiated HCCs and eight moderately differentiated HCCs exhibited washout within 1 minute after contrast administration (Table 2 and Fig. 3). Thirty-six lesions in addition to these 12 exhibited washout in the 5-minute phase: six poorly differentiated, 35 moderately differentiated, and seven well-differentiated HCCs, for a total of 48 lesions exhibiting washout in the 5-minute phase (Fig. 4). Similarly, because six lesions that did not exhibit washout in the 5-minute phase appeared as washout in the 10-minute



A

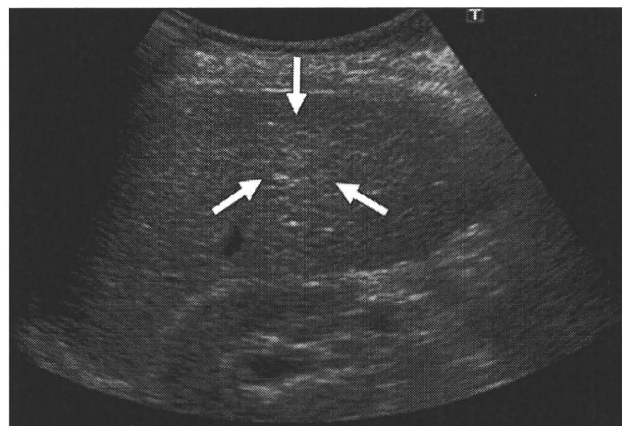


B

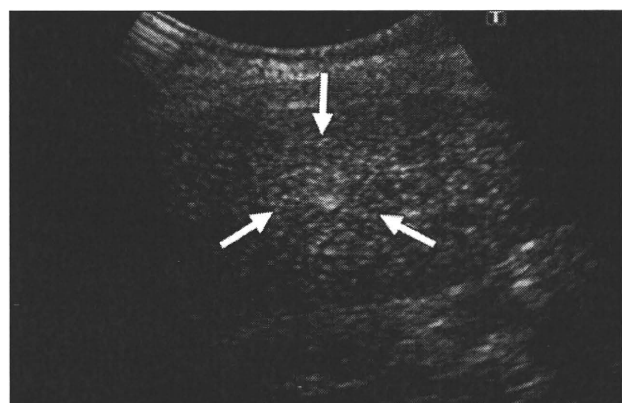


C

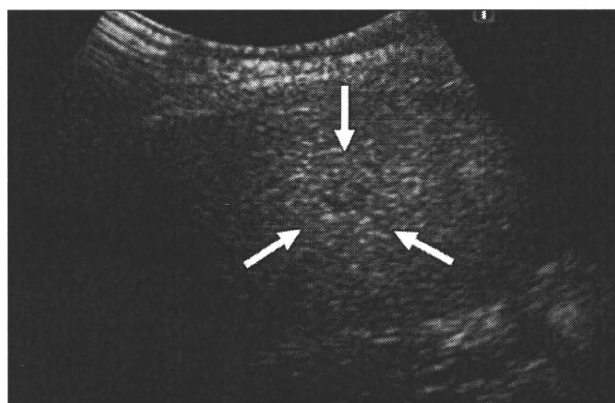
Fig. 3—62-year-old man with hepatitis B-related cirrhosis. **A**, Unenhanced sonogram shows hypoechoic 17.1-mm-diameter lesion (arrows) in liver. **B**, Contrast-enhanced sonogram at peak enhancement (31 seconds after injection) shows hyperenhancing lesion (arrows). **C**, Contrast-enhanced sonogram obtained in 1-minute phase (56 seconds after agent injection) shows hypoenhancing lesion (arrows), which was diagnosed as poorly differentiated hepatocellular carcinoma after ultrasound-guided needle biopsy.



A



B



C

Fig. 4—69-year-old woman with hepatitis C-related cirrhosis. **A**, Unenhanced sonogram shows 12.3-mm-diameter isoechoic lesion (arrows) in liver. **B**, Contrast-enhanced sonogram at peak enhancement (28 seconds after injection) shows hyperenhancing lesion (arrows). **C**, Contrast-enhanced sonogram obtained in 5-minute phase (5 minutes 4 seconds after injection) shows hypoechoic lesion (arrows), which was diagnosed as moderately differentiated hepatocellular carcinoma after ultrasound-guided needle biopsy.

phase, a total of 54 lesions exhibited washout in this final phase: six poorly differentiated HCCs, 38 moderately differentiated, and 10 well-differentiated HCCs. Washout was significantly more frequent for poorly differentiated HCC than for moderately differentiated HCC ($p = 0.0117$) or well-differentiated HCC ($p = 0.0003$) in the 1-minute phase and more frequent for moderately differentiated than for well-differentiated HCC in the 5-minute phase ($p = 0.0026$) and the 10-minute phase ($p = 0.0117$). The 10 lesions without washout in the 10-minute phase (four moderately differentiated and six well-differentiated HCCs) were isoenhancing (Fig. 5). Although three of the 11 lesions with isoenhancement at peak enhancement were moderately differentiated HCC, the other eight isoenhancing lesions and two hypoechoic lesions were well-differentiated HCC.

Discussion

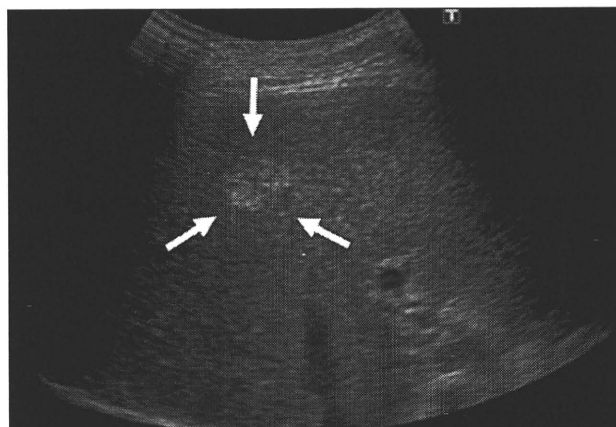
Step-by-step differentiation is the estimated natural progression of HCC [19, 20, 22,

23], and the changes in tumor appearance can be appreciated at imaging. As shown in our results, only poorly and moderately differentiated HCC exhibited washout within 1 minute, but the appearance was found predominantly in poorly differentiated HCC (66.7%). Cellular differentiation is a significant factor in prognosis and recurrence among HCC patients after liver transplant, and fine-needle biopsy of the tumor is recommended for pre-transplant workup [24]. In addition, because the risk of metastasis increases in cases of poorly differentiated HCC, evaluation of cellular differentiation affects patient care [25]. Noninvasive prediction of differentiation with perflutane microbubble-enhanced sonography should have considerable benefit in the clinical management of HCC.

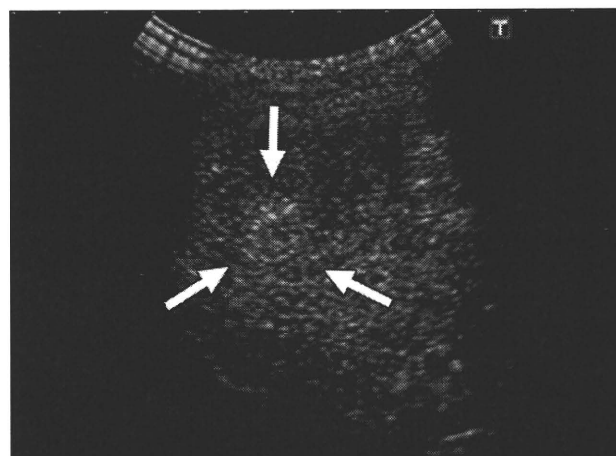
The sonographic shift of a hepatic tumor from hyperenhancement to hypoechoic according to imaging phase is a well-known phenomenon in contrast-enhanced ultrasound [12, 14, 26]. There are several explanations for the relation between cellular differentiation

and washout timing of perflutane microbubble-related contrast enhancement. First, the presence of Kupffer cells in the HCC lesion may account for the shift of washout timing. Studies have shown a relation between distribution of Kupffer cells in the HCC lesion and its cellular differentiation [27–29], and phagocytosis by Kupffer cells is one of the proposed mechanisms for accumulation of perflutane microbubbles in the liver [16, 17]. It remains to be elucidated, however, when accumulation of the microbubbles starts after the agent is injected and whether accumulated microbubbles play a role as a signal enhancer. Second, structural differences in the blood sinus in HCC lesions related to cellular differentiation may explain the difference in washout timing. That is, the greater the structural difference between sinusoids in adjacent liver parenchyma and the blood sinus in HCC becomes, the faster the passage of microbubbles in HCC. Results of some studies support this hypothesis. Using perflutren lipid microspheres (Definity, Lantheus Medical Imaging), a blood pool contrast

Ultrasound of Hepatocellular Carcinoma



A



B



C

Fig. 5—78-year-old man with hepatitis C–related cirrhosis.
A, Unenhanced sonogram shows 17.9-mm-diameter hyperechoic lesion (*arrows*) in liver.
B, Contrast-enhanced sonogram at peak enhancement (45 seconds after injection) shows hyperenhancing lesion (*arrows*).
C, Contrast-enhanced sonogram obtained in 10-minute phase (10 minutes 10 seconds after injection) shows isoenhancing lesion (*circle*), which was diagnosed as well-differentiated hepatocellular carcinoma after ultrasound-guided needle biopsy.

agent that does not accumulate in the liver, Jang et al. [30] found that earlier shift of washout time in HCC was related to tumor differentiation. They mentioned that total lack of similarity to the normal hepatocyte and its architecture in poorly differentiated HCC may be the explanation for the earliest washout time in the lesion. Nicolau et al. [31] reported that hypoenhancement with an aqueous suspension of phospholipid-stabilized microbubbles filled with sulfur hexafluoride (SonoVue, Bracco), which also is a blood pool contrast agent, was more frequent after the arterial phase of enhancement as differentiation of HCC progressed. Another study with aqueous suspension of phospholipid-stabilized microbubbles filled with sulfur hexafluoride also showed that hypovascularity in the portal venous phase was more frequent in moderately and poorly differentiated HCC than in well-differentiated HCC [32]. These results suggest that the earlier shift of washout time may be common in contrast-

enhanced ultrasound regardless of the type of agent, that is, with or without accumulation activity in the liver, although a continuous study may be necessary to prove this point.

Another aspect of washout in contrast-enhanced ultrasound is strong suspicion of a malignant lesion, whereas isoenhancement in the delayed phase seems to suggest a lesion is benign [14]. It has been reported [32] that differentiation between benign and malignant nodules measuring 2 cm or smaller that are hypervascular in the arterial phase and iso-vascular or hypervascular in the portal venous phase cannot be achieved with contrast-enhanced ultrasound because such findings are seen in both well-differentiated HCC and hypervascular benign nodules. Although our study did not include benign hepatic lesions, we emphasize that isoenhancement in the late phase does not always feature a benign lesion. In our study, 9.5% of moderately differentiated HCCs and 37.5% of well-differentiated

HCCs exhibited late phase iso-enhancement. Characterization of hepatic lesions without hypoenhancement after peak enhancement should be a future challenge.

The concordance rate between contrast-enhanced ultrasound and CTHA with respect to hyperenhancement was 98.4% (63/64). Discrepancy occurred in only one case: hyperenhancement at contrast-enhanced ultrasound and iso-enhancement at CTHA. Because it is believed that CTHA yields the highest rate of detection of tumor vascularity [33, 34], there is no standard imaging tool other than CTHA for judging contrast-enhanced ultrasound findings, and false-positive results of ultrasound cannot be denied. However, we emphasize that the rate of detection of tumor vascularity with contrast-enhanced ultrasound with the perflubutane microbubble agent was at least the same as that with CTHA. As previously discussed, CTHA requires an invasive procedure and

excessive radiation exposure [35]. Despite its operator- and patient-dependent nature, contrast-enhanced ultrasound with the perflubutane microbubble agent can be expected to be a standard method for assessment of tumor vascularity.

It has been reported [30] that there was no significant difference between the washout time of hypervascular HCC in noncirrhotic liver and that in severely fibrotic liver, although the differentiation of HCC in each group was not provided in the report. We speculated, however, that depending on the hemodynamics of the hepatic artery and portal vein and microbubble accumulation by the reticuloendothelial system, time-related changes in the contrast enhancement of HCC lesions may be affected by enhancement of adjacent hepatic parenchyma. Although all of the subjects in our study had cirrhosis, parenchymal enhancement itself might vary according to the severity of liver damage. We therefore based quantitative assessment of tumor enhancement on the intensity distribution in the nontumor area to minimize the effect of parenchymal enhancement. Objective assessment of contrast enhancement between HCC lesions and adjacent liver parenchyma showed excellent agreement with the results of subjective assessment in our study, although there were a few cases of disagreement in every phase. In addition, the results of intensity measurement showed sufficient interobserver and intraobserver variability for positioning ROIs, representing reliable procedure. However, because analysis of intensity can be complicated, an automatic measurement process should be introduced for assessment of the contrast-enhanced ultrasound findings.

There were shortcomings to our study. The first was that hepatic tumors comprised only HCC, not other tumors, such as cholangiocellular carcinoma, hypervascular metastatic liver cancer, hemangioma, and focal nodular hyperplasia. Because differential diagnosis between HCC and these liver tumors sometimes is required, time-related changes in contrast enhancement should be examined for these hepatic lesions. The second limitation was that our study included a small number of hypovascular and isovascular HCCs and no borderline lesions such as dysplastic nodules. Because most of the pathologic specimens were obtained by percutaneous needle biopsy with a 21-gauge needle, we cannot deny the difficulty of differentiation between dysplastic nodule and well-dif-

ferentiated HCC; some high-grade dysplastic nodules might have been classified as well-differentiated HCC. The third limitation was that we observed contrast enhancement only up to 10 minutes after contrast injection. Although observation for more than 10 minutes may not be practical, a previous report [21] showed the usefulness of contrast enhancement 30 minutes after injection in the assessment of cellular differentiation of HCC. The appropriate time for observation of contrast enhancement according to specific purpose should be established in the near future.

We conclude that the washout time of perflubutane microbubble-related contrast enhancement in HCC lesions was closely related to cellular differentiation of HCC. Although further studies involving a large patient sample may be necessary to confirm the results, we believe our technique has potential for obviating needle biopsy in the assessment of cellular differentiation of HCC.

References

- Llovet JM, Burroughs A, Bruix J. Hepatocellular carcinoma. *Lancet* 2003; 362:1907–1917
- Bruix J, Llovet JM. Prognostic prediction and treatment strategy in hepatocellular carcinoma. *Hepatology* 2002; 35:519–524
- Carr BI. Hepatocellular carcinoma: current management and future trends. *Gastroenterology* 2004; 127:S218–S224
- Asayama Y, Yoshimitsu K, Nishihara Y, et al. Arterial blood supply of hepatocellular carcinoma and histologic grading: radiologic-pathologic correlation. *AJR* 2008; 190:90; [web]W28–W34
- Bruix J, Sherman M, Llovet JM, et al. Clinical management of hepatocellular carcinoma; conclusions of the Barcelona-2000 EASL conference. European Association for the Study of the Liver. *J Hepatol* 2001; 35:421–430
- Murakami T, Kim T, Takamura M, et al. Hypervascular hepatocellular carcinoma: detection with double arterial phase multi-detector row helical CT. *Radiology* 2001; 218:763–767
- Bolondi L, Gaiani S, Celli N, et al. Characterization of small nodules in cirrhosis by assessment of vascularity: the problem of hypovascular hepatocellular carcinoma. *Hepatology* 2005; 42:27–34
- Roncalli M, Roz E, Coggi G, et al. The vascular profile of regenerative and dysplastic nodules of the cirrhotic liver: implications for diagnosis and classification. *Hepatology* 1999; 30:1174–1178
- Matsui O, Kadoya M, Kameyama T, et al. Benign and malignant nodules in cirrhotic livers: distinction based on blood supply. *Radiology* 1991; 178:493–497
- Takayasu K, Muramatsu Y, Furukawa H, et al. Early hepatocellular carcinoma: appearance at CT during arterial portography and CT arteriography with pathologic correlation. *Radiology* 1995; 194:101–105
- Giorgio A, Ferraioli G, Tarantino L, et al. Contrast-enhanced sonographic appearance of hepatocellular carcinoma in patients with cirrhosis: comparison with contrast-enhanced helical CT appearance. *AJR* 2004; 183:1319–1326
- Lencioni R; European Federation of Societies for Ultrasound in Medicine and Biology (EFSUMB). Impact of European Federation of Societies for Ultrasound in Medicine and Biology (EFSUMB) guidelines on the use of contrast agents in liver ultrasound. *Eur Radiol* 2006; 16:1610–1613
- Maruyama H, Takahashi M, Ishibashi H, et al. Ultrasound-guided treatments under low acoustic power contrast harmonic imaging for hepatocellular carcinomas undetected by B-mode ultrasonography. *Liver Int* 2009; 29:708–714
- Quaia E, Calliada F, Bertolotto M, et al. Characterization of focal liver lesions with contrast-specific US modes and a sulfur hexafluoride-filled microbubble contrast agent: diagnostic performance and confidence. *Radiology* 2004; 232:420–430
- Wilson SR, Burns PN, Muradali D, Wilson JA, Lai X. Harmonic hepatic US with microbubble contrast agent: initial experience showing improved characterization of hemangioma, hepatocellular carcinoma, and metastasis. *Radiology* 2000; 215:153–161
- Watanabe R, Matsumura M, Chen CJ, Kaneda Y, Fujimaki M. Characterization of tumor imaging with microbubble-based ultrasound contrast agent, Sonazoid, in rabbit liver. *Biol Pharm Bull* 2005; 28:972–977
- Marelli C. Preliminary experience with NC100100, a new ultrasound contrast agent for intravenous injection. *Eur Radiol* 1999; 9[suppl 3]:S343–S346
- Kojiro M. Focus on dysplastic nodules and early hepatocellular carcinoma: an Eastern point of view. *Liver Transpl* 2004; 10:S3–S8
- Sakamoto M, Hirohashi S, Shimosato Y. Early stages of multistep hepatocarcinogenesis: adenomatous hyperplasia and early hepatocellular carcinoma. *Hum Pathol* 1991; 22:172–178
- Takayama T, Makuuchi M, Hirohashi S, et al. Malignant transformation of adenomatous hyperplasia to hepatocellular carcinoma. *Lancet* 1990; 336:1150–1153
- Korenaga K, Korenaga M, Furukawa M, Yamasaki T, Sakaida I. Usefulness of Sonazoid contrast-enhanced ultrasonography for hepatocellular carcinoma: comparison with pathological diagnosis and superparamagnetic iron oxide magnetic resonance images. *J Gastroenterol* 2009; 44:733–741

Ultrasound of Hepatocellular Carcinoma

22. Kojiro M, Nakashima O. Histopathologic evaluation of hepatocellular carcinoma with special reference to small early stage tumors. *Semin Liver Dis* 1999; 19:287–296
23. Oikawa T, Ojima H, Yamasaki S, Takayama T, Hirohashi S, Sakamoto M. Multistep and multicentric development of hepatocellular carcinoma: histological analysis of 980 resected nodules. *J Hepatol* 2005; 42:225–229
24. Zavaglia C, De Carlis L, Alberti AB, et al. Predictors of long-term survival after liver transplantation for hepatocellular carcinoma. *Am J Gastroenterol* 2005; 100:2708–2716
25. Si MS, Amersi F, Golish SR, et al. Prevalence of metastases in hepatocellular carcinoma: risk factors and impact on survival. *Am Surg* 2003; 69:879–885
26. Gaiani S, Celli N, Piscaglia F, et al. Usefulness of contrast-enhanced perfusional sonography in the assessment of hepatocellular carcinoma hypervascular at spiral computed tomography. *J Hepatol* 2004; 41:421–426
27. Imai Y, Murakami T, Yoshida S, et al. Superparamagnetic iron oxide-enhanced magnetic resonance images of hepatocellular carcinoma: correlation with histological grading. *Hepatology* 2000; 32:205–212
28. Inoue T, Kudo M, Watai R, et al. Differential diagnosis of nodular lesions in cirrhotic liver by post-vascular phase contrast-enhanced US with Levovist: comparison with superparamagnetic iron oxide magnetic resonance images. *J Gastroenterol* 2005; 40:1139–1147
29. Tanaka M, Nakashima O, Wada Y, Kage M, Kojiro M. Pathomorphological study of Kupffer cells in hepatocellular carcinoma and hyperplastic nodular lesions in the liver. *Hepatology* 1996; 24:807–812
30. Jang HJ, Kim TK, Burns PN, Wilson SR. Enhancement patterns of hepatocellular carcinoma at contrast-enhanced US: comparison with histologic differentiation. *Radiology* 2007; 244:898–906
31. Nicolau C, Catala V, Vilana R, et al. Evaluation of hepatocellular carcinoma using SonoVue, a second generation ultrasound contrast agent: correlation with cellular differentiation. *Eur Radiol* 2004; 14:1092–1099
32. Quaia E, D'Onofrio M, Cabassa P, et al. Diagnostic value of hepatocellular nodule vascularity after microbubble injection for characterizing malignancy in patients with cirrhosis. *AJR* 2007; 189:1474–1483
33. Irie T, Takeshita K, Wada Y, et al. CT evaluation of hepatic tumors: comparison of CT with arterial portography, CT with infusion hepatic arteriography, and simultaneous use of both techniques. *AJR* 1995; 164:1407–1412
34. Kanematsu M, Hoshi H, Murakami T, et al. Detection of hepatocellular carcinoma in patients with cirrhosis: MR imaging versus angiographically assisted helical CT. *AJR* 1997; 169:1507–1515
35. Chezmar JL, Bernardino ME, Kaufman SH, Nelson RC. Combined CT arterial portography and CT hepatic angiography for evaluation of the hepatic resection candidate: work in progress. *Radiology* 1993; 189:407–410



Increased Serum Levels of Pigment Epithelium-Derived Factor by Excessive Alcohol Consumption—Detection and Identification by a Three-Step Serum Proteome Analysis

Kazuyuki Sogawa, Yoshio Kodera, Mamoru Satoh, Yusuke Kawashima, Hiroshi Umemura, Katsuya Maruyama, Hirotaka Takizawa, Osamu Yokosuka, and Fumio Nomura

Background: The search for biological markers of alcohol abuse is of continual interest in experimental and clinical alcohol research. We previously used gel-free proteome analysis methods such as the ProteinChip[®] system and the ClinProt[™] system to search for new serum markers for alcoholism and found several novel marker candidates. As serum contains thousands of proteins and peptides that are present in a large dynamic concentration, depletion of the abundant proteins and further fractionation of the remainder is necessary to get into the deep proteome. We recently described a simple and highly reproducible three-step method for identifying potential disease-marker candidates among the low-abundance serum proteins.

Methods: Two serum samples—one on admission and one after 8 weeks of abstinence—were obtained from 8 patients with alcohol dependency. The samples were subjected to a three-step serum proteome analysis. The steps were the following: first, immunodepletion of the 6 most abundant proteins; second, fractionation using reverse-phase high-performance liquid chromatography; and third, separation using one-dimensional sodium dodecyl sulfate polyacrylamide gel electrophoresis (SDS-PAGE). Differences revealed by protein staining were further confirmed by Western blotting and by enzyme-linked immunosorbent assays (ELISA).

Results: Three-step serum proteome analysis revealed that the serum levels of 5 proteins, alpha2-HS glycoprotein, apolipoprotein A-I, glutathione peroxidase 3, heparin cofactor II, and pigment epithelial-derived factor (PEDF), were significantly greater on admission than after 8 weeks of abstinence. We focused on PEDF because alterations in its levels in alcoholic subjects are not well known. Western blotting and ELISA confirmed the upregulation of PEDF. Serum PEDF levels were significantly greater in moderate to heavy habitual drinkers ($14.2 \pm 7.7 \mu\text{g/ml}$) than in healthy subjects without a drinking history ($5.5 \pm 3.0 \mu\text{g/ml}$) ($p < 0.001$). The serum PEDF levels in subjects with nonalcoholic chronic liver diseases were comparable to the PEDF levels in healthy subjects.

Conclusion: Three-step serum proteome analysis reveals that excessive alcohol drinking increases the PEDF level.

Key Words: Alcoholism, Pigment Epithelial-Derived Factor, Proteomics, Serum.

EXCESSIVE ALCOHOL CONSUMPTION causes alcoholism and alcoholic liver diseases and aggravates many common medical problems such as hypertension,

diabetes mellitus, and gout. Although the primary strategy for detecting heavy drinking relies on self-reporting, heavy drinkers tend to underestimate their alcohol consumption. This leads to an underdiagnosis of hazardous alcohol use and related disorders (Alling et al., 2005). Therefore, the search for biological markers of alcohol abuse is of continual interest in experimental and clinical alcohol research (Hannuksela et al., 2007; Niemela, 2007; Nomura et al., 2007).

We previously used the ProteinChip[®] system to search for new serum markers of alcoholism and found several novel marker candidates (Nomura et al., 2004). Of these markers, a 5.9-kDa peptide (which is a fragment of the fibrinogen alpha chain) with an m/z of 5890 was useful in detecting gamma-glutamyltransferase (GGT) nonresponders in male subjects seeking a medical checkup (Sogawa et al., 2007). More recently, we used the ClinProt[™] system (Bruker Daltonics, Bremen, Germany; consisting of a combination of beads processing and matrix-assisted laser desorption/ionization

From the Clinical Proteomics Research Center (KS, YK, MS, YK, FN), Chiba University Hospital, Chiba, Japan; Department of Physics (YK), School of Science, Kitasato University, Kanagawa, Japan; Department of Molecular Diagnosis (HU, FN), Graduate School of Medicine, Chiba University, Chiba, Japan; National Hospital Organization Kurihama Alcoholism Center (KM), Kanagawa, Japan; Kashiwado Clinic in Port-Square (HT), Kashiwado Memorial Foundation, Chiba, Japan; and Division of Gastroenterology (OY), Chiba University Hospital, Chiba, Japan.

Received for publication April 26, 2010; accepted July 18, 2010.

Reprint requests: Fumio Nomura, MD, PhD, Department of Molecular Diagnosis, Graduate School of Medicine, Chiba University, 1-8-1 Inohana, Chuo-ku, Chiba City, Chiba 260-8670, Japan; Fax: +81-43-226-2324; E-mail: fnomura@faculty.chiba-u.jp

Copyright © 2010 by the Research Society on Alcoholism.

DOI: 10.1111/j.1530-0277.2010.01336.x

Alcohol Clin Exp Res, Vol 35, No 2, 2011; pp 211–217

211

time-of-flight mass spectroscopy [MALDI-TOF MS]) to facilitate close analysis of serum peptide markers not detectable by the ProteinChip[®] system. We found 4 other peaks as candidate peptide markers (Sogawa et al., 2009).

A technical challenge in serum proteome analysis is that serum contains thousands of proteins and peptides that are present in a large dynamic concentration. Indeed, 22 abundant proteins such as albumin, immunoglobulins, and transferrin constitute up to 99% of the protein content of plasma (Anderson and Anderson, 2002; Tirumalai et al., 2003). Depletion of these abundant proteins and further fractionation of samples will be necessary in future proteomic studies searching for low-abundance serum proteins or peptides.

We recently described a simple and highly reproducible three-step method for identifying potential disease-marker candidates among the low-abundance serum proteins (Kawashima et al., 2009). Using this method, we successfully identified 3 proteins, including YKL-50, as promising biomarkers of sepsis (Hattori et al., 2009). The three steps are the following: first, immunodepletion of the abundant proteins; second, fractionation using reverse-phase high-performance liquid chromatography (HPLC); and third, one-dimensional sodium dodecyl sulfate polyacrylamide gel electrophoresis (SDS-PAGE). In this study, we applied this three-step proteome analysis method to gain more insight into the alterations of serum proteins resulting from excessive alcohol consumption. We detected and identified increased pigment epithelial-derived factor (PEDF) serum levels after excessive alcohol consumption.

MATERIALS AND METHODS

Patients

Sequential serum samples were obtained from patients with alcohol dependency on admission and after 8 weeks of abstinence. The patients were diagnosed in accordance with the DSM IV criteria (American Psychiatric Association, 1994) and admitted to the National Hospital Organization Kurihama Alcoholism Center (Kanagawa, Japan). All of the patients consumed more than 100 g of alcohol per day for more than 10 years until the day of hospitalization.

A total of 120 patients with biopsy-proven nonalcoholic liver diseases were included. In this group, 20 patients had chronic hepatitis

B; 20 patients had liver cirrhosis because of hepatitis B virus (HBV) infection; 20 patients had chronic hepatitis C; 20 patients had liver cirrhosis because of hepatitis C virus (HCV) infection; 20 patients had autoimmune hepatitis; and 20 patients had primary biliary cirrhosis.

Blood samples were also obtained from 60 apparently healthy subjects with various drinking habits who visited the Kashiwado Clinic in Port-Square of Kashiwado Memorial Foundation (Chiba, Japan) for their annual medical checkup. All subjects were administered a detailed questionnaire concerning the amount of alcoholic beverages consumed (calculated as grams of ethanol per day), the duration of drinking, and the frequency of drinking. Twenty nondrinkers, 20 light drinkers (less than 40 g/d), and 20 heavy drinkers (more than 80 g/d) were randomly selected from subjects who sought a medical checkup. These subgroups were defined by the criteria reported by Conigrave and colleagues (2002).

The demographic data of the subjects studied are presented in Table 1.

All the serum samples were collected, processed in a protocol that we previously described (Umehura et al., 2009), and stored at -80°C in aliquots until analysis. All of the subjects provided written informed consent, and the Ethics Committee of Chiba University School of Medicine approved this study.

The Removal of High-Abundance Proteins From the Serum Samples

The first step of the three-step analysis involved removing the 6 major serum proteins—albumin, immunoglobulin G, alpha-1-antitrypsin, immunoglobulin A, transferrin, and haptoglobin—by passing them through a commercially available immunoaffinity column, the Multi Affinity Removal column (Agilent Technologies Inc., Santa Clara, CA). Twenty-five microliters of serum was diluted to 75 μL with a loading buffer (Agilent Technologies Inc.) and spin-filtered (0.22 μm) for 30 min at 13,000 rpm and 4°C . One hundred microliters of each sample was injected from an autosampler cooled to 4°C . Depletion was performed at room temperature on a Shimadzu LC10A VP HPLC system (Shimadzu Co., Kyoto, Japan), using the following program: 9 min at 100% eluent A (Agilent Technologies Inc.) at 0.25 ml/min; 3.5 min at 100% eluent B (Agilent Technologies Inc.) at 1.0 ml/min; and then 7.5 min at 100% eluent A at 1.0 ml/min. Based on the chromatogram, which was recorded by measuring the absorbance of the eluate at 280 nm, the flow-through fractions eluted at a retention time between 2.5 min and 6.5 min were collected in eight 0.125 mL aliquots (for a total volume of 1.0 ml). Using Vivaspin 2 Polyethersulfone spin concentrators (molecular weight cutoff at 10 kDa; Vivascience, Hannover, Germany), the flow-through fractions were combined and concentrated by centrifugal ultrafiltration to a total volume of 80 μL . The concentrated sample solution was stored at -80°C until use.

Table 1. Demographic Data of Subjects Studied

Experimental diseases (number of patients)	Sex (M/F)	Age (mean \pm SD)	Alcohol consumption (mean \pm SD g/d)
Alcohol dependency ($n = 20$)	20/0	52.8 \pm 11.9	201.3 \pm 57.3
Healthy volunteers			
Nondrinkers ($n = 20$)	20/0	50.9 \pm 9.0	—
Low-risk drinkers ($n = 20$)	20/0	50.0 \pm 5.3	30.0 \pm 6.2
High-risk drinkers ($n = 20$)	20/0	50.4 \pm 6.5	107.5 \pm 35.2
Nonalcoholic liver disease			
Hepatitis B virus infection			
Chronic hepatitis ($n = 20$)	10/10	49.2 \pm 14.6	—
Liver cirrhosis ($n = 20$)	10/10	61.6 \pm 9.3	—
Hepatitis C virus infection			
Chronic hepatitis ($n = 20$)	12/8	63.9 \pm 14.6	—
Liver cirrhosis ($n = 20$)	12/8	69.4 \pm 8.5	—
Autoimmune hepatitis ($n = 20$)	4/16	61.7 \pm 15.3	—
Primary biliary cirrhosis ($n = 20$)	4/16	63.2 \pm 8.3	—

Reverse-Phase High-Performance Liquid Chromatography

The second step of the three-step analysis involved subjecting the concentrated flow-through fractions (75 μ L) to the Intradra WP-RP column (Imtakt, Kyoto, Japan), which was attached to an HPLC system (NANOSPACE SI-2 system; Shiseido Fine Chemicals, Tokyo, Japan). We conducted chromatography, as previously described (Kawashima et al., 2009). Each fraction was dried in a centrifugal vacuum concentrator and stored at -80°C for subsequent SDS-PAGE analysis.

SDS-PAGE Analysis

The third step of the three-step analysis involved subjecting each HPLC fraction to SDS-PAGE. The lyophilized samples of the HPLC fractions were dissolved in a PAGE sample buffer (pH 6.8; 50 mM Tris-HCl, 50 mM dithiothreitol, 0.5% SDS and 10% glycerol). The solution was then analyzed using SDS-PAGE (Perfect NT Gel W, 10 to 20% acrylamide, 20 wells; DRC Co., Ltd., Tokyo, Japan) in accordance with the manufacturer's protocol. The gel was stained with Coomassie brilliant blue (CBB) (PhastGel Blue R; GE Healthcare, Little Chalfont, UK). TotalLab TL120 software v2006 (Shimadzu Co.) quantified the intensity of each protein band, and the intensity was used as an index of the level of protein expression. The protein bands were excised from the gel; in-gel tryptic digestion was performed and the protein was identified, as we previously described (Hattori et al., 2009).

Western Blotting

The protein extracts were separated by electrophoresis on 10 to 20% gradient gels (DRC Co., Ltd.). The proteins were transferred to polyvinylidene fluoride membranes (Millipore Corporate Headquarters, Billerica, MA) in a tank-transfer apparatus (Bio-Rad

Laboratories, Hercules, CA). The membranes were blocked with 5% skim milk in phosphate-buffered saline (PBS). Mouse anti-PEDF (TransGenic Inc., Hyogo, Japan) diluted 1:250 in blocking buffer was used as the primary antibody. Peroxidase-conjugated AffiniPure goat anti-mouse IgG (H + L) (Jackson ImmunoResearch Laboratories Inc., West Grove, PA) diluted 1:1,000 in blocking buffer was used as the secondary antibody. Enhanced chemiluminescence detection reagents (GE Healthcare, Buckinghamshire, UK) detected the antigens on the membrane. TotalLab TL120 software v2006 (Shimadzu Co.) quantified the intensity of each protein band; the intensity was used as an index of the level of protein expression.

Other Procedures

Serum levels of PEDF were determined by enzyme-linked immunosorbent assay (ELISAquant™ PEDF Sandwich ELISA Antigen Detection Kit [BioProducts MD, Middletown, MD]). Numerical data are presented as the mean \pm standard deviation (SD). We evaluated the statistical significance using IBM SPSS Statistics 18 software (SPSS Inc., Chicago, IL). *p* Values less than 0.05 were considered significant.

RESULTS

Three-Step Proteome Analyses

Two serum samples from each of the 8 patients with alcohol abuse—one sample obtained on admission and the second, after 8 weeks of abstinence—were subjected to three-step serum proteome analysis. A representative CBB-stained SDS-PAGE gel (fraction No. 14) is shown in Fig. 1A. After converting the intensity of each band to a numerical value

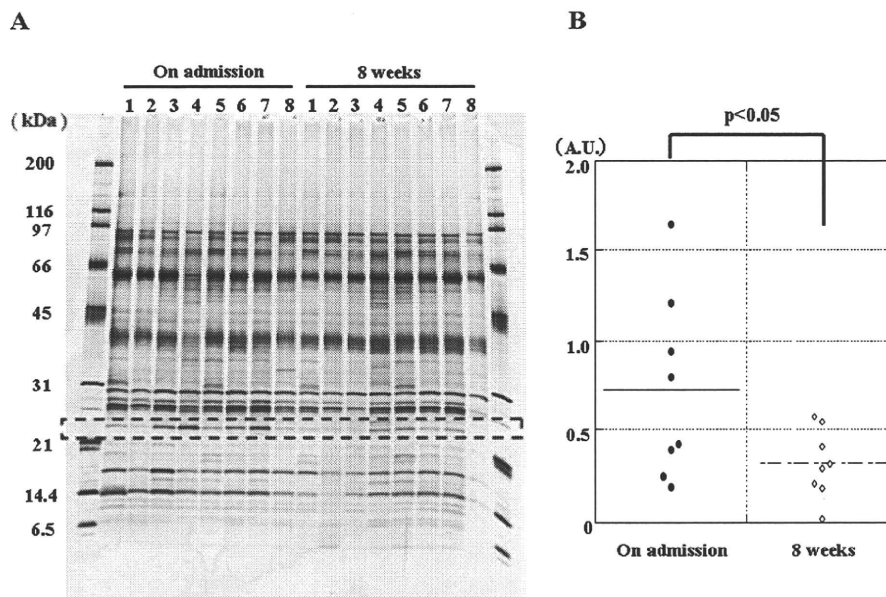


Fig. 1. Representative SDS-PAGE gel of an RP-HPLC fraction (fraction No. 14) and the comparison of the band intensities, as assessed by densitometry. Serum samples (100 μ L each) were immunodepleted and injected onto the RP-HPLC column. Proteins in each fraction were subjected to 10 to 20% SDS-PAGE, as described in Methods. Following electrophoresis, the proteins were visualized using CBB staining. The image indicates the 25-kDa band that is equivalent to PEDF (A). The expression level of the 25 kDa band was quantified using densitometry in the 8 pairs of samples (i.e., 16 samples). The difference in the PEDF expression level is statistically significant (B). CBB, coomassie brilliant blue; ELISA, enzyme-linked immunosorbent assay; PEDF, pigment epithelial-derived factor; RP-HPLC, reverse-phase high-performance liquid chromatography; SDS-PAGE, sodium dodecyl sulfate polyacrylamide gel electrophoresis.

Table 2. Serum Proteins Upregulated (A) and Downregulated (B) in Alcoholic Patients on Admission, as Detected by Three-Step Proteome Analysis

No.	Database accession no.	ID	MW	Score	Number of matching peptides	Sequence coverage (%)
A. Upregulated serum proteins						
1	gi2521981	Alpha2-HS glycoprotein	35,641	112	5	8
2	gi90108664	Apolipoprotein A-I	28,061	1,409	43	70
3	gi121672	Glutathione peroxidase 3	25,489	82	2	6
4	gi23200172	Heparin cofactor II	57,034	161	3	5
5	gi189778	PEDF	46,300	491	9	22
B. Downregulated serum proteins						
1	gi224917	Apolipoprotein C-III	8,759	118	3	24

MW, molecular weight; PEDF, pigment epithelial-derived factor.

(using TotalLab TL120 software v2006), the 8 pairs of samples showed a significant difference in the expression level of the 25 kDa band on admission and after 8 weeks of abstinence from drink ($p < 0.05$) (Fig. 1B). A comparison of all 40 RP-HPLC fractions revealed that the expression levels of 27 bands at the time of admission changed significantly after 8 weeks abstinence from drink ($p < 0.01$). On admission, 24 bands were upregulated and three bands were downregulated.

Identification of Protein

Of the 27 bands, 6 bands, which demonstrated particularly remarkable changes, were digested by trypsin and were subjected to tandem mass spectrometry for identification. The 6 proteins that were identified are listed in Table 2. The 5 proteins that were upregulated on admission were alpha2-HS

glycoprotein, apolipoprotein A-I, glutathione peroxidase 3, heparin cofactor II, and PEDF (Table 2A). The protein band that was downregulated on admission was apolipoprotein C-III (Table 2B).

Western Blotting

Of the 5 proteins upregulated on admission, we focused on PEDF mainly because the alteration in the levels of this protein because of heavy drinking is not well known. The results obtained by SDS-PAGE were confirmed by Western blotting performed on the same 8 pairs of serum samples subjected to the three-step proteome analysis (Fig. 2A). A semi-quantitative analysis of the results, using the TotalLab TL120 software, revealed a statistically significant difference between the serum PEDF level on admission and after 8 weeks of abstinence from drink ($p < 0.05$) (Fig. 2B).

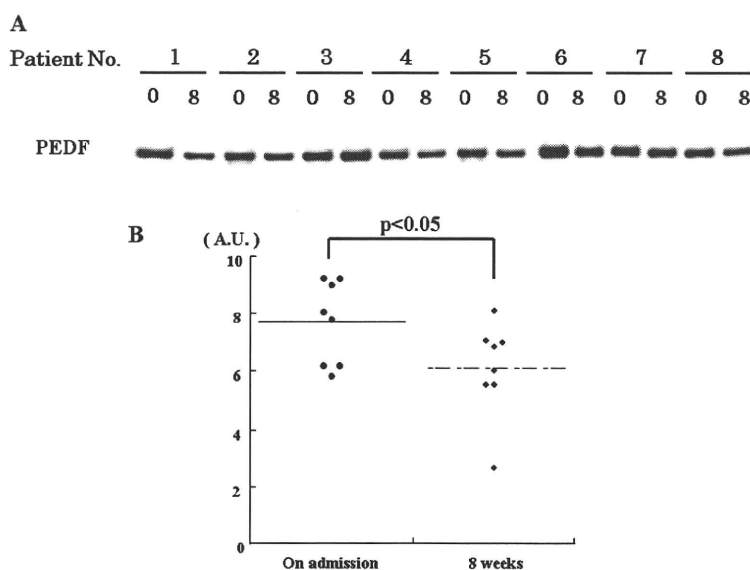


Fig. 2. Western blot analysis of PEDF in the serum samples of the alcoholic patients. (A) The 8 sample pairs of the immunodepleted sera, which had been obtained from alcoholic patients on admission (week 0) and after 8 weeks of abstinence (week 8). The serum samples were separated using 10 to 12% SDS-PAGE and probed with anti-PEDF antibody, as described in Methods. (B) The densitometric comparison of the bands' intensities. The PEDF expression level is significantly greater on admission than after 8 weeks of abstinence ($p < 0.05$). PEDF, pigment epithelial-derived factor; SDS-PAGE, sodium dodecyl sulfate polyacrylamide gel electrophoresis.